Published in final edited form as:
J Med Chem. 2008 September 25; 51(18): 5608–5616. doi:10.1021/jm800329z.

Discovery and Labeling of High Affinity 3,4-Diarylpyrazolines as Candidate Radioligands for *In Vivo* Imaging of Cannabinoid Subtype-1 (CB_1) Receptors

Sean R. Donohue[1,2,*], **Victor W. Pike**[1], **Sjoerd J. Finnema**[2], **Phong Truong**[2], **Jan Andersson**[2], **Balázs Gulyás**[2], and **Christer Halldin**[2]

[1]Molecular Imaging Branch, National Institute of Mental Health, National Institutes of Health, Bethesda, MD 20892, USA

[2]Karolinska Institutet, Department of Clinical Neuroscience, Psychiatry Section, Karolinska Hospital, S-17176 Stockholm, Sweden

Abstract

Imaging of cannabinoid subtype-1 (CB_1) receptors *in vivo* with positron emission tomography (PET) is likely to be important for understanding their role in neuropsychiatric disorders and for drug development. Radioligands for imaging with PET are required for this purpose. We synthesized new ligands from a 3,4-diarylpyrazoline platform of which (-)-**12a** ((-)-3-(4-chlorophenyl)-*N'*-[(4-cyanophenyl)sulfonyl]-4-phenyl-4,5-dihydro-1*H*-pyrazole-1-carboxamidine) was found to have high-affinity and selectivity for binding to CB_1 receptors. (-)-**12a** and its lower affinity enantiomer ((+)-**12a**) were labeled with carbon-11 ($t_{1/2}$ = 20.4 min) using [^{11}C]cyanide ion as labeling agent and evaluated as PET radioligands in cynomolgus monkey. After injection of [^{11}C](-)-**12a** there was high uptake and retention of radioactivity across brain according to the rank order of CB_1 receptor densities. The distomer, [^{11}C](+)-**12a**, failed to give a sustained CB_1 receptor-specific distribution. Polar radiometabolites of [^{11}C](-)-**12a** appeared moderately slowly in plasma. Radioligand [^{11}C](-)-**12a** is promising for the study of brain CB_1 receptors and merits further investigation in human subjects.

Introduction

The psychotropic, analgesic and healing properties of *Cannabis sativa* (marijuana) have been known throughout documented history.1 As for some other plant-derived medications (*e.g*., opium), there has been significant abuse of marijuana mainly because of an accompanying feeling of relaxation and psychological "high".2,3 Nevertheless, legitimate medical use of marijuana may extend to the treatment of chemotherapy-induced emesis,4,5 appetite stimulation in acquired immune deficiency syndrome (AIDS)6,7 and movement disorders caused by multiple sclerosis8,9.

*Author for correspondence. Address: Molecular Imaging Branch, National Institute of Mental Health, National Institutes of Health, Building 10, Rm B3 C342, 10 Center Drive, Bethesda, MD 20892-1003, USA (Tel. 1-301-451-3909, Fax. 1-301-480-5112); email.donohues@intra.nimh.nih.gov.

Efforts to elucidate the biological response to marijuana intake have identified (-)-(6a*R*, 10a*R*)-6,6,9-trimethyl-3-pentyl-6a,7,8,10a-tetrahydro-6*H*-benzo[*c*]chromen-1-ol, **1** (Δ^9-THC, Figure 1)10,11, as its most abundant active compound. **1** interacts with two main receptor types, namely cannabinoid subtype-1 (CB_1) and cannabinoid subtype-2 (CB_2) receptors.12,13 Two spliced variants of the CB_1 receptor have also been identified, CB_{1A} and CB_{1B}.14,15 CB_1 receptors are located throughout the body and have high densities in regions of the brain, such as the hippocampus, striatum and basal ganglia.16,17 By contrast, CB_2 receptors are located mainly in peripheral tissues and are associated with the immune system.13,18,19

In 1994 Sanofi-Synthlabo introduced 5-(4-chlorophenyl)-1-(2,4-dichloro-phenyl)-4-methyl-*N*-(piperidin-1-yl)-1*H*-pyrazole-3-carboxamide, **2** (SR141716A, rimonabant, Figure 1), as a high-affinity inverse agonist at CB_1 receptors.20 **2** has recently gained approval for use in the European Union as a treatment for morbid obesity. The therapeutic use of **2** may extend to addiction and neurodegenerative disorders. Consequently, there has been a considerable effort by pharmaceutical industry to develop novel CB_1 receptor inverse agonist platforms. Solvay AB succeeded with the development of (4*S*)-3-(4-chlorophenyl)-*N*-methyl-*N'*-[(4-chlorophenyl)sulfonyl]-4-phenyl-4,5-dihydro-1*H*-pyrazole-1-carboxamidine, **3** (SLV319, Figure 1).21-23

Brain CB_1 receptors may be involved in several neuropsychiatric disorders. Currently, there is a need for suitable ligands that are amenable to labeling with positron-emitters for non-invasively imaging CB_1 receptors *in vivo* with PET under control and diseased states. Previous attempts at radioligand development have focused on the modification of the 1,5-diarylpyrazole CB_1 receptor class of **2** to allow for labeling with carbon-11 ($t_{1/2}$ = 20.4 min), fluorine-18 ($t_{1/2}$ = 109.7 min) or iodine-124 ($t_{1/2}$ = 4.15 d). Some success has been achieved with this approach (Figure 2), namely through the development of [^{11}C]**4** ([^{11}C]JHU75528)24,25 and [^{11}C]**5** ([^{11}C]JHU75575)25. Promising PET radioligands from other structural platforms have recently been reported (Figure 2), such as [^{11}C]**6** ([^{11}C]PipISB),26 [^{18}F]**6** ([^{18}F]PipISB),26 [^{18}F]**7** ([^{18}F]MK-9760)27,28 and [^{11}C]**8** ([^{11}C]MePPEP)29.

A 3,4-diarylpyrazoline class of CB_1 receptor ligand also presents favorable physiological and pharmacological attributes for PET radioligand development. The lead structure (**3**) shows high selectivity and potency for CB_1 receptors with little to no substrate behavior for P-glycoprotein (P-gp) efflux pumps.22 Nevertheless, this structural class has remained largely unexplored for PET radioligand development. With this purpose in mind, we have synthesized novel analogs of **3** that are amenable to radiolabeling. The CB_1 receptor affinities (K_i values) and selectivities were determined for the enantiomers of two ligands that were considered amenable to labeling with carbon-11 or radioiodine (*e.g.*, iodine-123, $t_{1/2}$ = 13.13 h, or iodine-124). Additionally, one racemic ligand (**12a**), along with its eutomer and distomer, were labeled in high-specific radioactivity with [^{11}C]cyanide ion and investigated in monkey with PET imaging. The emergence of radiometabolites in monkey plasma was measured with HPLC.

Results and Discussion

Chemistry

Ligands (**12a-c**) were synthesized by modifications of known general procedures (Scheme 1).22 Briefly, the appropriate 4-substituted benzenesulfonamides (**9a-c**) were treated with methyl chloroformate plus triethylamine in acetonitrile to give the corresponding carbamic acid methyl esters (**10a-c**), which were then treated with 3-(4-chlorophenyl)-4,5-dihydro-4-phenyl-1*H*-pyrazole in toluene to give **11a-c** in good yields. Treatment of **11a-c** with PCl_5 in chlorobenzene gave the crude imino chlorides, which were readily converted with methanolic NH_3 into the target ligands, **12a-c**. These ligands were then resolved into their enantiomers with chiral HPLC.

CB_1 and CB_2 *in vitro* binding assays

High-affinity is a prerequisite in candidate radioligands for PET imaging of neuroreceptors.30 Generally, the more sparse the receptor the higher the affinity must be to permit successful imaging. As a guide, binding potentials represented by B_{max}/K_d should well exceed unity, when B_{max} and K_d (or as surrogate, K_i or IC_{50}) are expressed in nM.30 CB_1 receptors are amongst the most abundant receptors in brain16,17, and hence moderately high-affinity (K_i < 10 nM) may be acceptable. The IC_{50} and K_i values of rimonabant, (-)-**12a**, (+)-**12a**, (-)-**12c** and (+)-**12c** are shown in Table 1. The (-)-enantiomers exhibited high affinities for CB_1 receptors with IC_{50} values and K_is in low or sub nM range, respectively. These values compare well with other successful radioligands targeting CB_1 receptors, which generally have potencies or affinities in the nM range (*e.g.*, [^{18}F]**7** and [^{11}C]**8**). The (+)-enantiomers of **12a** and **12c** exhibited lower CB_1 receptor affinities than their (-)-enantiomers; eudismic ratios were found to be about 35 for **12a** and 56 for **12c**. These ratios are similar to those of similar CB_1 receptor ligands from the 3,4-diarylpyrazoline class.22 The eutomer of one such ligand has been shown to have the *S* configuration by X-ray crystallography.22 Hence, the eutomers of **12a** and **12c** are also predicted to have *S* configuration.

Receptor screening

Ligand (-)-**12a** showed < 50% inhibition (n = 4) for the following receptors and binding sites: 5-HT_{1A-E}, 5-HT_{2B-C}, 5-HT_3, 5-HT_{5A}, 5-HT_6, 5-HT_7, $\alpha_{1A,B}$, α_{2A-C}, β_{1-3}, D_{1-5}, DAT, DOR, $H_{1,4}$, KOR, M_{1-5}, MOR, NET, SERT, $\sigma_{1,2}$. K_i values (n = 3) of > 7,710 ± 1,110 nM for the 5-HT_{2A} and > 10,000 nM for $H_{2,3}$ receptors were found. Hence, (-)-**12a** was found to have excellent CB_1 receptor selectivity for development as a PET radioligand.

Lipophilicities

The lipophilicity of a radioligand may critically influence its ability to penetrate the blood-brain barrier. Generally, a Log*P* value in the range 2.0 to 3.5 is considered desirable for adequate brain entry without excessive non-specific binding to brain tissue (*i.e.*, fats, proteins).31 cLog*P* is a useful tool for predicting lipophilicity trends among compounds of the same structural class.30,31 cLog*P* was computed for (-)-**12a**, (+)-**12a**, (-)-**12c** and (+)-**12c** (Table 1). Ligand **3** has previously been shown to penetrate the blood-brain barrier, despite its very high cLog*P* value (5.01).22 The cLog*P* values of **12a** and its enantiomers are substantially lower (3.85) than that of **3** (Table 1), and hence they may be expected to enter brain readily. The values for **12c** and its enantiomers are similar to **3** and hence they may also be expected to enter brain adequately.

Radiosynthesis

Initially, we set out to find an effective and rapid method for labeling **12** as its racemate. [^{11}C]Cyanide ion is a useful precursor for ^{11}C-labeling molecules with an aryl nitrile group. 32 The incorporation of [^{11}C]cyanide ion into an aryl ring is best achieved with copper33,34 or palladium32 catalyzed reactions. We considered each method for labeling (±)-**12a**. At first glance, [^{11}C]Cu(I)CN appears attractive for labeling PET radiopharmaceuticals. In general, use of this labeling agent requires one-pot and is insensitive to H_2O or NH_3 accompanying the production of [^{11}C]HCN. However, the overall radiochemical yields can be very low (e.g., 2.5%), and inferior to those from the palladium-catalyzed method.34 Hence, the latter method was selected for labeling (±)-**12a**.

[^{11}C]HCN, which itself was prepared from cyclotron produced [^{11}C]methane, was trapped in a DMSO solution of KOH, and 4,7,13,16,21,24-hexaoxa-1,10-diazabicyclo[8.8.8]hexacosane (K 2.2.2) yielding a [^{11}C]CN^--K^+-K 2.2.2. complex, which was then added to the bromo precursor ((±)-**12b**) and $Pd(PPh_3)_4$ in DMSO and heated (Scheme 2). [^{11}C](±)-**12a** was separated from the crude product with reverse phase HPLC. The fraction containing [^{11}C](±)-**12a** was evaporated to dryness and formulated for safe intravenous injection. The overall radiosynthesis time was about 30 min. The non-optimized decay-corrected yield was 36% (*n* = 2). There was no great improvement in yield when using the iodo compound (-)-**12c** as precursor. [^{11}C](±)-**12a** was obtained in high radiochemical purity (> 98%) and was free of labeling precursors. Specific radioactivities were ≥ 56 GBq/μmol at time of injection. Product identity was confirmed by liguid chromatography-mass spectrometry (LC-MS) of associated carrier and by co-injection with **12** in HPLC analysis and observation of co-elution.

We attempted to prepare [^{11}C](-)-**12a** from precursor (-)-**12b** under the reaction conditions used to prepare [^{11}C](±)-**12a**. However, chiral HPLC analyses of the collected radioactive products revealed that complete racemization had occurred during the reactions (Table 2). Racemization was likely promoted by the strong base (KOH plus K 2.2.2) (Scheme 3).

To try to avoid racemization, several weaker bases were used in place of the KOH plus K 2.2.2. Interestingly, the use of $NaHCO_3$ as base gave, [^{11}C](-)-**12a** to [^{11}C](+)-**12a** in a 9: 1 ratio. Serendipitously, we found that the use of KH_2PO_4 (Table 2) gave [^{11}C](-)-**12a** in > 94% ee (*n* = 4). These conditions were also used with (+)-**12c** as precursor and the resulting product, [^{11}C](+)-**12a**, was obtained in > 94% ee. The chemical identities of [^{11}C](-)-**12a** and [^{11}C](+)-**12a** were confirmed with LC-MS of associated carrier. Thus, [^{11}C](-)-**12a** and [^{11}C](+)-**12a** were obtained in high-chiral purity for evaluation as radioligands in monkeys with PET.

PET measurements

After intravenous injection of [^{11}C](±)-**12a** into cynomolgus monkey, the brain radioactivity distributed according to the rank order of regional CB_1 receptor densities (Panel A, Figure 3). The highest radioactivity uptake was in CB_1 receptor-rich striatum, reaching 220% SUV at 30 min after injection. This slowly diminished to 180% SUV at 90 min after injection. The lowest maximal brain uptake was in pons reaching 150% SUV at 24 min after injection. The concentration of radioactivity in this region diminished to 124% SUV at 90 min after injection. In an experiment in which the CB_1 receptor-selective ligand **6** was given in high dose (1 mg/kg, i.v.) at 25 min after injection of [^{11}C](±)-**12a**, the regional brain radioactivity became homogeneous and diminished to about 95% SUV at 90 min after injection (Panel B, Figure 3). When **6** (1 mg/kg, i.v.) was given at 20 min before injection of [^{11}C](±)-**12a**, brain radioactivity became homogenous and was characterized by a lower maximal uptake and fast washout, reaching 175% SUV at 15 min after injection and declining to 85% SUV at 90 min after injection (Panel C, Figure. 3). These results demonstrated that a high proportion of brain radioactivity in the baseline experiment was reversibly bound to CB_1 receptors. The higher affinity enantiomer in this racemic radioligand was expected to be responsible for the majority of receptor-specific binding, while the lower affinity enantiomer was expected to bind mostly non-specifically. We therefore set out to inject the homochiral radioligands, [^{11}C](-)-**12a** and [^{11}C](+)-**12a**, to test these expectations.

After intravenous injection of the higher affinity enantiomer, [^{11}C](-)-**12a**, into monkey, the brain radioactivity again distributed according to the regional rank order of CB_1 receptor densities. The highest uptake of radioactivity was in striatum, reaching 200% SUV at 48 min after injection. The lowest maximal brain uptake was in pons reaching and maintaining ~ 125% SUV from 24 min after injection (Panel A, Figure 4). These time-activity curves are consistent with a high proportion of receptor-specific binding in all examined brain regions, as also seen in the experiment with racemic radioligand (Panel A, Figure 3).

In these experiments, as in PET imaging studies of other CB_1 receptor radioligands,27,29 no region could be identified to represent non-specific binding only. Pons does not serve this purpose, since it contains some CB_1 receptors16,17,27 and measurements of its radioactivity concentration are contaminated from other nearby regions (*e.g.*, CB_1 receptor-rich cerebellum) through the partial volume effect. In the absence of a reference region, ratios of specific to non-specific binding cannot be estimated at all accurately by visual inspection of time-activity curves. Bolus plus constant infusion35 or full kinetic compartmental model utilizing an arterial input function would be required to extract this information.29

By contrast with results from [^{11}C](-)-**12a**, after intravenous injection of the lower affinity enantiomer, [^{11}C](+)-**12a**, into monkey, maximal brain radioactivity concentration reached 280% SUV at 1.5 min, but then rapidly declined in all regions to about 95% SUV at 90 min (Panel B, Figure 4). These features of the time-activity curves are consistent with a high proportion of non-specific binding in all examined regions, and are consistent with the lower affinity of the radioligand.

Horizontal PET images obtained at the level of the striatum from data acquired between 9 and 93 min after injection of [^{11}C](-)-**12a** showed a distribution of radioactivity consistent with a large proportion of specific binding to CB_1 receptors, whereas corresponding images obtained with [^{11}C](+)-**12a** were strikingly homogeneous indicating little receptor-specific binding.

Emergence of radiometabolites of [^{11}C](-)-12a in plasma

Analysis of venous samples showed that after injection of [^{11}C](-)-**12a** into cynomolgus monkey, three less lipophilic radiometabolite fractions (t_Rs = 2.3, 5.8 and 8 min, *cf.* t_R = 8.5 min for [^{11}C](-)-**12a**) emerged in plasma (Panel A, Figure 6). Unchanged radioligand had declined to 50% of radioactivity in plasma at 45 min after injection (Panel B, Figure 6). The presence of the three radiometabolite fractions slowly increased as a percentage of total radioactivity in plasma throughout the scan. In this study, we did not determine the identities of any of these radiometabolite fractions nor whether they crossed the blood-brain barrier.

Finally, (-)-**12c** was not labeled with radioiodine in this study, but its properties (high-affinity, high-selectivity and lipophilicity) suggest it has potential for development as a radioligand for imaging brain CB_1 receptors, either for PET or SPECT.

Conclusions

3,4-Diarylpyrazoline CB_1 ligands with high-affinity and selectivity for CB_1 receptors were discovered. One racemic ligand ((±)-**12a**), its eutomer ((-)-**12a**) and its distomer ((+)-**12a**) were successfully labeled with carbon-11 in high specific radioactivity. [^{11}C](-)-**12a** was found to be a promising radioligand for PET receptor imaging and merits further exploration in humans.

Experimental Section

Materials

All reagents were of ACS or HPLC quality and purchased from commercial sources, and were used as received. 4-Cyanophenylsulfonamide, 4-bromophenylsulfonamide and 4-iodophenylsulfonamide were synthesized by known procedures.36 3-(4-Chlorophenyl)-4,5-dihydro-4-phenyl-1*H*-pyrazole was also synthesized as reported.37 **6** was provided by Eli Lilly and Co.

General methods

^{1}H (400 MHz) and ^{13}C (100 MHz) NMR spectra were recorded at room temperature on an Avance-400 spectrometer (Brucker; Billerica, MA). Chemical shifts are reported in δ units (ppm) downfield relative to the chemical shift for tetramethylsilane. Signals are quoted as s (singlet), d (doublet), dd (double doublet), dt (double triplet), t (triplet), q (quartet) or m (multiplet). High-resolution mass spectra (HRMS) were determined using a time-of-flight electrospray instrument (University of Illinois at Urbana, Champaign, IL, USA). Melting points (mp) were determined using a Mel-temp melting point apparatus (Electrothermal, Fisher Scientific, USA) and were uncorrected. Chiral HPLC, for the preparative resolution of racemates to enantiomers, was performed on a chiral column (ChiralPak AD, 20 × 250 mm) eluted with acetonitrile at 6 or 8 mL/min, as later specified. The enantiomeric excess (ee) of each resolved compound was measured by HPLC with the same method as used for resolution. Optical rotations $\left([\alpha]_D^{22}\right)$ were measured with a P-1010 polarimeter (JASCO; Easton, MD). Specific rotations were obtained at room temperature. Mass spectra (MS) were acquired using a LCQ^{DECA} LC-MS instrument (Thermo Finnigan; San Jose, CA, USA) fitted with a reverse phase LC column (Luna, C18; 5 µm, 2 × 150 mm; Phenomenex). Radiosyntheses were performed in a custom-made remotely-controlled apparatus.38 Radioligand separations were performed with HPLC on a reverse phase column (µ-Bondapak C-18; 7.8 × 300 mm, 10 µm; Waters). The column outlet was connected to an absorbance detector (λ = 254 nm) in series with a GM-tube for radiation detection. [^{11}C](±)-**12a**, [^{11}C](-)-**12a** and [^{11}C](+)-**12a** were purified in this system using MeCN-0.01 M H_3PO_4 (55: 45, v/v) as mobile phase at 6 mL/min. The radiochemical purities and specific radioactivities of each product were determined with reverse phase HPLC on a µ-Bondapak C-18 column (3.9 × 300 mm, 10 µm; Waters) eluted at 3 mL/min with MeCN-H_3PO_4 (0.01 M; 55: 45 v/v) as mobile phase. Eluate was monitored with an absorbance detector (λ = 254 nm) in series with a β-flow detector (Beckman) for radiation detection. The enantiomeric excess of each labeled product was measured by chiral HPLC, as described above; eluate was monitored for absorbance and radioactivity. Specific radioactivities (GBq/µmol) were determined with analytical HPLC calibrated for absorbance (λ = 254 nm) response per mass of ligand. The specific radioactivity was calculated as the radioactivity of the radioligand peak (decay-corrected) (GBq) divided by the mass of the associated carrier peak (µmol). The metabolism of [^{11}C](-)-**12a** was assessed with HPLC on a reverse phase (µ-Bondapak C-18 column; 7.8 × 300 mm, 10 µm; Waters) eluted at 6 mL/min with a gradient of MeCN (A) and *aq*-H_3PO_4 (0.01 M) (B), with A increasing linearly from 35 to 65% v/v for 6 min and then to 35% v/v over the next 2 min and then held for 4 min. The column outlet was connected to an absorbance detector (λ = 270 nm) in series with a GM-tube for radiation detection.

N-[(4-Cyanophenyl)sulfonyl]carbamic acid methyl ester (10a)

Methyl chloroformate (6.34 mL, 82.4 mmol) was slowly added to a stirred solution of 4-cyanobenzenesulfonamide (10 g, 54.9 mmol) and triethylamine (23 mL, 165 mmol) in acetonitrile (75 mL). The reaction was stirred at room temperature for 16 h and then evaporated to dryness *in vacuo*. After addition of ethyl acetate and *aq*. $NaHCO_3$ to the crude residue, the aqueous layer was separated and acidified. The oily precipitate crystallized on standing and was filtered off, washed with water and dried to give **10a** (6.9 g, 52% yield); mp 130-132 °C; ^{1}H NMR (400 MHz, $CDCl_3$): δ 3.72 (s, 3H), 7.87 (2H, dt, J = 9.0, 2.0 Hz), 8.19 (2H, dt, J = 8.8, 2.0 Hz), NH proton invisible.

N-[(4-Bromophenyl)sulfonyl]carbamic acid methyl ester (10b)

10b was prepared from 4-bromobenzenesulfonamide in 48% yield by the method described for **10a**; mp 120-122 °C; ^{1}H NMR (400 MHz, $CDCl_3$): δ 3.72 (s, 3H), 7.71 (2H, dt, J = 8.8, 2.0 Hz), 7.93 (2H, dt, J = 8.8, 2.0 Hz), NH proton invisible.

N-[(4-Iodophenyl)sulfonyl]carbamic acid methyl ester (10c)

10c was prepared from 4-iodoobenzenesulfonamide in 56% yield by the method described for **10a**; mp 116-118 °C; ^{1}H NMR (400.13 MHz, $CDCl_3$): δ 3.72 (s, 3H), 7.77 (2H, dt, *J* = 8.8, 2.0 Hz), 7.93 (2H, dt, *J* = 8.8, 2.0 Hz), NH proton invisible.

3-(4-Chlorophenyl)-N-[(4-cyanophenyl)sulfonyl]-4-phenyl-4,5-dihydro-1H-pyrazole-1-carboxamide (11a)

To a solution of 3-(4-chlorophenyl)-4,5-dihydro-4-phenyl-1*H*-pyrazole (6.4 g, 25.4 mmol) in toluene (100 mL) was added **10a** (6.1 g, 25.4 mmol) and the resulting solution was heated to reflux for 2 h. After cooling to room temperature, **11a** began to crystallize slowly from solution. The crystals were filtered off and washed twice with MTBE to give pure **11a** (9.2 g, 78% yield); mp 208-210 °C; ^{1}H NMR (400 MHz, $CDCl_3$): δ 3.92 (1H, dd, *J* = 6.2, 5.2 Hz), 4.34 (1H, t, *J* = 4.3 Hz), 4.75 (1H, dd, *J* = 6.2, 5.2 Hz), 7.12 (2H, dt, *J* = 6.6, 1.6 Hz), 7.33-7.24 (5H, m), 7.55 (2H, dt, *J* = 8.6, 1.8 Hz), 7.86 (2H, dt, *J* = 8.6, 1.8 Hz), 8.30 (2H, dt, *J* = 8.6, 1.8 Hz), 8.8 (1H, bs); ^{13}C NMR (100 MHz, $CDCl_3$): δ 51.54, 54.02, 117.39, 127.21, 127.92, 128.25, 128.74, 129.08, 129.23, 129.61, 132.72, 136.85, 138.93, 143.06, 147.55, 156.82; LC-MS m/z (M^+ + H) = 464.9; HRMS calcd for $C_{23}H_{18}N_4O_3SCl$ (M^+ + H), 465.0788; found, 465.0774; error (ppm): - 3.0.

3-(4-Chlorophenyl)-*N*-[(4-bromophenyl)sulfonyl]-4-phenyl-4,5-dihydro-1H-pyrazole-1-carboxamide (11b)

11b was prepared from 3-(4-chlorophenyl)-4,5-dihydro-4-phenyl-1*H*-pyrazole and **10b** in 82% yield by the method described for **11a**; mp 214-216 °C; ^{1}H NMR (400 MHz, $CDCl_3$): δ 3.92 (1H, dd, *J* = 6.2, 5.2 Hz), 4.34 (1H, t, *J* = 4.3 Hz), 4.75 (1H, dd, *J* = 6.2, 5.2 Hz), 7.12 (2H, dt, *J* = 6.6, 1.6 Hz), 7.33-7.24 (5H, m), 7.55 (2H, dt, *J* = 8.6, 1.8 Hz), 7.71 (2H, dt, *J* = 8.6, 1.8 Hz), 8.04 (2H, dt, *J* = 8.6, 1.8 Hz), 8.76 (1H, s); ^{13}C NMR (100.62 MHz, DMSO-d_6): δ 21.02, 49.43, 54.53, 101.86, 125.28, 127.25, 127.48, 128.17, 128.56, 128.87, 129.06, 129.17, 129.26, 134.69, 137.31, 137.92, 138.16, 139.59, 140.15, 148.52, 155.89; LC-MS m/z (M^+ + H) = 519.9; HRMS calcd for $C_{22}H_{18}N_3O_3SClBr$ (M^+ + H), 517.9941; found 517.9929; error (ppm): - 2.3.

3-(4-Chlorophenyl)-N-[(4-iodophenyl)sulfonyl]-4-phenyl-4,5-dihydro-1H-pyrazole-1-carboxamide (11c)

11c was prepared from 3-(4-chlorophenyl)-4,5-dihydro-4-phenyl-1*H*-pyrazole and **10c** in 74.5% yield by the method described for **11a**; mp 212-214 °C; ^{1}H NMR (400 MHz, $CDCl_3$): δ 3.92 (1H, dd, *J* = 6.2, 5.2 Hz), 4.34 (1H, t, *J* = 4.3 Hz), 4.73 (1H, dd, *J* = 6.1, 5.2 Hz), 7.16 (2H, dt, *J* = 6.6, 1.6 Hz), 7.33-7.24 (5H, m), 7.55 (2H, dt, *J* = 8.7, 2.0 Hz), 7.71 (4H, qt, *J* = 9.8, 8.8, 1.8 Hz), 8.8 (1H, s); ^{13}C NMR (100.62 MHz, $CDCl_3$): δ 51.5, 54.0, 127.2, 128.1, 128.2, 128.3, 128.7, 129.1, 129.6, 129.9, 132.3, 136.7, 138.1, 139.1, 147.8, 156.4; LC-MS m/z (M^+ + H) = 565.8; HRMS calcd for $C_{22}H_{18}N_3O_3SClI$ (M^+ + H), 565.9802; found: 565.9801; error (ppm): - 0.2.

3-(4-Chlorophenyl)-*N*'-[(4-cyanophenyl)sulfonyl]-4-phenyl-4,5-dihydro-1H-pyrazole-1-carboxamidine (12a)

A mixture of **11a** (6 g, 12.9 mmol) and PCl_5 (2.8 g, 13.5 mmol) was dissolved in chlorobenzene (80 mL), refluxed for 1 h and then concentrated *in vacuo*. The residue was treated with methanolic NH_3 (1 M, 5 mL). The mixture was stirred at room temperature for 1 h and then concentrated *in vacuo*. The product was recrystallized from MeOH to give **12a** (2.2 g, 37%); mp 208-210 °C; ^{1}H NMR (400.13 MHz, $CDCl_3$): δ 4.02 (dd, J = 12.0, 4.0 Hz, 1H), 4.42 (t, J = 12.0 Hz, 1H), 4.76 (dd, J = 12.0, 4.0 Hz, 1H), 7.10 (dt, J = 6.4, 2.0 Hz, 2H), 7.34-2.25 (m, 3H), 7.55 (dt, J = 8.7, 2.0 Hz, 2H), 7.6 (d, J = 8.0 Hz, 2H), 7.75 (dt, J = 8.6, 1.4 Hz, 2H), 8.05 (dt, J = 8.6, 1.4 Hz, 2H); ^{13}C NMR (100.62 MHz, $CDCl_3$): δ 51.42, 55.34, 115.29, 117.77, 126.87, 127.18, 128.04, 128.22, 128.69, 129.09, 129.61, 132.58, 136.89, 138.93, 147.60, 152.72, 158.05; LC-MS m/z (M^+ + H), 464.0; HRMS calcd for $C_{23}H_{19}N_5O_2SCl$ (M^+ + H), 464.0948; found, 464.0957; error (ppm): 1.9.

(-)-3-(4-Chlorophenyl)-*N*'-[(4-cyanophenyl)sulfonyl]-4-phenyl-4,5-dihydro-1*H*-pyrazole-1-carboxamidine ((-)-12a)

Resolution of **12a** by chiral HPLC (see General Methods) gave (-)-**12a** (t = 9.8 min at 8 mL/min, > 98% ee); $\left([\alpha]_D^{22}\right)$ = - 69.3°, c = 0.010, CH_2Cl_2; mp 208-210 °C; ^{1}H-NMR: as found for **12a**; MS m/z (M^+ + H), 464.1; HRMS, calcd for $C_{23}H_{19}N_5O_2SCl$ (M^+ + H), 464.0948; found, 464.0962; error (ppm): 3.0; Anal. ($C_{23}H_{18}ClN_5O_2S$) C, H, N.

(+)-3-(4-Chlorophenyl)-N'-[(4-cyanophenyl)sulfonyl]-4-phenyl-4,5-dihydro-1H-pyrazole-1-carboxamidine ((+)-12a)

Resolution of **12a** by chiral HPLC (see General Methods) gave (+)**-12a** (t_R = 12.27 min at 8 mL/min, > 98% ee); $\left([\alpha]_D^{22}\right)$ = + 66.3°, c = 0.011, CH_2Cl_2; mp 208-210 °C; ^{1}H-NMR: as found for **12a**; MS m/z (M^+ + H) 464.1; HRMS calcd for $C_{23}H_{19}N_5O_2SCl$ (M^+ + H) 464.0948; found, 464.0961, error (ppm): 2.8; Anal. ($C_{23}H_{18}ClN_5O_2S$) C, H, N.

3-(4-Chlorophenyl)-*N*'-[(4-bromophenyl)sulfonyl]-4-phenyl-4,5-dihydro-1*H*-pyrazole-1-carboxamidine (12b)

12b was prepared from **11b** in 43% yield by the method described for **12a**; mp 214-216 °C; ^{1}H NMR (400.13 MHz, DMSO-d_6): δ 3.80 (1H, dd, J = 6.6, 4.7 Hz), 4.37 (1H, t, J = 11.5 Hz), 5.04 (1H, dd, J = 6.6, 4.7 Hz), 7.16 (2H, d, J = 7.1 Hz), 7.25 (1H, t, J = 7.2 Hz), 7.35 (2H, t, J = 7.6 Hz), 7.44 (2H, d, J = 8.6 Hz), 7.76 (2H, d, J = 8.4 Hz), 7.79-7.71 (2H, m); ^{13}C NMR (100.62 MHz, DMSO-d_6) δ 49.62, 55.60, 125.22, 127.20, 127.52, 127.85, 128.60, 128.83, 129.12, 129.21, 131.83, 134.92, 140.05, 142.96, 152.76, 157.60; LC-MS m/z $[M + H]^+$ 517.0; HRMS calcd for $C_{22}H_{19}N_4O_2SClBr$ (M^+ + H), 517.0101; found, 517.0117, error (ppm): 3.1.

(-)-3-(4-Chlorophenyl)-*N*'-[(4-bromophenyl)sulfonyl]-4-phenyl-4,5-dihydro-1*H*-pyrazole-1-carboxamidine ((-)-12b)

Resolution of **12b** by chiral HPLC (see General Methods) gave (-)-**12b** (t_R = 13.78 min at 8 mL/min, > 98% ee); $\left([\alpha]_D^{22}\right)$ = - 65.7°, c = 0.010, CH_2Cl_2; mp 214-216 °C; ^{1}H NMR: as found for **12b**; MS m/z (M^+ + H) 517.0. HRMS calcd for $C_{22}H_{19}N_4O_2SClBr$ (M^+ + H) 517.0101, found: 517.0126, error (ppm): 4.8.

(+)-3-(4-Chlorophenyl)-*N*'-[(4-bromophenyl)sulfonyl]-4-phenyl-4,5-dihydro-1*H*-pyrazole-1-carboxamidine ((+)-12b)

Resolution of **12b** by chiral HPLC (see General Methods) gave (+)-**12b** (t_R = 18.14 min at 8 mL/min, > 98% ee); $\left([\alpha]_D^{22}\right)$ = 65.2°, c = 0.010, CH_2Cl_2; mp 214-216 °C; ^{1}H NMR: as found for **12b**; MS m/z (M^+ + H) 517.0; HRMS calcd for $C_{22}H_{19}N_4O_2SClBr$ (M^+ + H) 517.0101, found: 517.0110, error (ppm): 1.7.

3-(4-Chlorophenyl)-*N*'-[(4-iodophenyl)sulfonyl]-4-phenyl-4,5-dihydro-1*H*-pyrazole-1-carboxamidine (12c)

12c was prepared from **11c** in 64% yield by the method described for **12a**; mp 222-224 °C; ^{1}H NMR (400 MHz, DMSO-d_6): δ 3.80 (1H, dd, J = 6.6, 4.7 Hz), 4.37 (1H, t, J = 11.5 Hz), 5.04 (1H, dd, J = 6.6, 4.7 Hz), 7.18 (2H, d, J = 7.1 Hz), 7.26 (1H t, J = 7.2 Hz), 7.35 (2H, t, J = 7.6 Hz), 7.44 (2H, d, J = 8.6 Hz), 7.62 (2H, d, J = 8.4 Hz), 7.77 (2H, d, J = 8.6 Hz), 7.90 (2H, d, J = 8.4 Hz); ^{13}C NMR (100.62 MHz, DMSO-d_6): δ 49.60, 55.59, 99.28, 127.19, 127.52, 127.59, 128.69, 128.83, 129.11, 129.21, 134.92, 137.65, 140.05, 143.30, 152.74, 157.57; LC-MS m/z (M^+ + H) 565.1; HRMS calcd for $C_{22}H_{19}N_4O_2SClI$ (M^+ + H) 564.9962, found: 564.9974, error (ppm): 2.1.

(-)-3-(4-Chlorophenyl)-*N*'-[(4-iodophenyl)sulfonyl]-4-phenyl-4,5-dihydro-1*H*-pyrazole-1-carboxamidine ((-)-12c)

Resolution of **12c** by chiral HPLC (see General Methods) gave (-)-**12c** (t_R = 18.18 min at 6 mL/min, > 98% ee); $\left([\alpha]_D^{22}\right)$ = - 160°, c = 0.011, $CHCl_3$; mp 222-224 °C; ^{1}H NMR: as found for **12c**; LC-MS m/z (M^+ + H) 565.1; HRMS calcd for $C_{22}H_{19}N_4O_2SClI$ (M^+ + H): 564.9962, found: 564.9960, error (ppm): - 0.4.; Anal.. ($C_{22}H_{18}ClIN_4O_2S$) C, H, N.

(+)-3-(4-Chlorophenyl)-*N*'-[(4-iodophenyl)sulfonyl]-4-phenyl-4,5-dihydro-1*H*-pyrazole-1-carboxamidine ((+)-12c)

Resolution of **12c** by chiral HPLC (see General Methods) gave (+)-**12c** (t_R = 24.38 min at 6 mL/min, > 98% ee); $\left([\alpha]_D^{22}\right)$ = + 151°, c = 0.010, $CHCl_3$; mp 222-224 °C; ^{1}H NMR: as found for **12c**; LC-MS m/z (M^+ + H) 565.0; HRMS calcd for $C_{22}H_{19}N_4O_2SClI$ (M^+ + H) 564.9962, found: 564.9960, error (ppm): - 0.4; Anal.. ($C_{22}H_{18}ClIN_4O_2S$) C, H, N.

CB_1 and CB_2 Binding assays

Frozen cell membranes (recombinant hCB1r or hCB2r; Perkin Elmer) were thawed and diluted (7 μg/well) in membrane buffer (final concentrations: 100 mM NaCl, 5 mM $MgCl_2$, 1 mM EDTA, 50 mM HEPES, 10 μM GDP, 100 μM DTT, 0.01% fatty acid free BSA).

[^{35}S]GTPγS was diluted with distilled water to a final concentration of 0.5 nM. The inhibitory effect of test ligands was measured against a concentration (EC_{80}) of the CB1r/CB2r agonist CP-55,940 (Tocris) added to the solution.

Membrane solution (100 μL) and radioligand solution (100 μL) were added to the assay plates together with 2 μL compound (concentration-response in DMSO) and incubated for 45 min at 30 °C. Bound [^{35}S]GTPγS was separated from free [^{35}S]GTPγS by rapid filtration under vacuum through Whatman GF/B glass fiber filters, followed by washes with cold wash solution (final concentration: 50 mM Tris, 5 mM $MgCl_2$, 50 mM NaCl). The filters were dried for 60 min at 50 °C. Scintillation film was melted onto the filters, which were then counted in a Microbeta scintillation counter. Non-specific binding was determined in the presence of a saturating concentration of GTPγS (final concentration 20 μM). IC_{50} values were converted to K_i values according to the Cheng and Prusoff equation.39 The data represent K_i ± SD (nM) from triplicate determinations vs. CB1r or CB2r

Receptor screening

Ligand (-)-**12a** was screened for binding to a wide range of receptors and transporters by the National Institute of Mental Health Psychoactive Drug Screening Program. Detailed protocols are available on-line for all binding assays at the NIMH-PDSP web site (http://pdsp.med.unc.edu).

[^{11}C]HCN production

[^{11}C]Methane was produced at the Karolinska Hospital with a GEMS PETtrace cyclotron using 16.4 MeV protons in the ^{14}N(p,α)^{11}C reaction on N_2(g) containing 10% H_2(g).40 The target gas was irradiated for 5 min with a beam intensity of 35μA. The [^{11}C]methane was isolated from the target gas in a Porapak Q trap, which was cooled with N_2(l). The Porapak Q trap was warmed and the [^{11}C]methane passed in nitrogen (200 mL/min) with NH_3(g) (20-30 mL/min) over heated (990 °C) Pt wire (1.3 g, 0.127 mm, 99%; Sigma Aldrich) in a quartz tube within a carbolite furnace (MTF 10/15). The resulting [^{11}C]NH_4CN was bubbled through *aq*. 50% H_2SO_4 (2 mL) at 56 °C to generate [^{11}C]HCN.

Radiosyntheses of [^{11}C](±)-12a, [^{11}C](-)-12a and [^{11}C](+)-12a

The generated [^{11}C]HCN (~ 12.4 GBq) was trapped in a V-vial (5-mL) containing DMSO (400 μL) base (KOH, 1 mg, 17.8 μmol; K 2.2.2., 5 mg, 13.3 μmol) for [^{11}C](±)-**12a** or KH_2PO_4 (1 mg, 7.34 μmol) for [^{11}C](-)-**12a** or [^{11}C](+)-**12a**. After trapping of [^{11}C]HCN was complete, the solution was transferred into another V-vial (10 mL) which contained DMSO (400 μL), $Pd(PPh_3)_4$ (5.5 mg, 4.8 μmol) and the requisite precursor ((±)-**12b**, (-)-**12b**, (-)-**12c** or (+)-**12c**; 1 mg). The reaction was heated 135 °C for 4 min and then cooled to room temperature. HPLC mobile phase (800 μL) was added to the V-vial and the radioactive product separated with HPLC (see General Methods). The radioactive fraction

(t_R = 12.3 min) was collected, evaporated to dryness, and taken up in ethanol-propylene glycol (30: 70 v/v, 3 mL) with sterile phosphate buffer (0.2 M, pH = 7.4, 5 mL) and filtered through a sterile filter (Millex GV, 0.22 μm pore size; Millipore Corp., Corrigtwohill, Co. Cork, Ireland).41 A sample (100 ∼ μL) was analyzed by HPLC for radiochemical purity and measurement of specific radioactivity (see General methods).

PET measurements in monkey

Cynomolgus monkey (*Macaca fascicularis*) experiments were performed at the Karolinska Institutet (KI) according to "Guidelines for planning, conducting and documenting experimental research" (Dnr 4820/06-600) of the KI as well as the "Guide for the Care and Use of Laboratory Animals".42 The study was approved by the Animal Ethics Committee of the Swedish Animal Welfare Agency. Two cynomolgus monkeys (3.4 and 4.8 kg) were used in the PET experiments. Anesthesia was induced and maintained with repeated i.m. injections of a mixture of ketamine hydrochloride (3.75 mg/kg^{-1} h^{-1} Ketalar®, Pfizer) and xylazine hydrochloride (1.5 mg/kg^{-1} h^{-1} Rompun® Vet., Bayer). The head for each monkey was immobilized in a stereotactic frame for the duration of scans.43 The body temperature was maintained by a Bair Hugger Model 505 (Arizant Healthcare, MN, USA) and monitored by rectal thermometer (Precision Thermometer, Harvard Apparatus, MA, USA).

In baseline experiments, each radioligand was administered by bolus injection over about 5 s, with injected activities of 56, 100, and 98 MBq and specific radioactivities of 78, 65, and 56 GBq/μmol for [^{11}C](±)-**12a**, [^{11}C](-)-**12a** and [^{11}C](+)-**12a**, respectively. The masses of injected carrier ligand were 0.33 μg (0.72 nmol), 0.71 μg (1.53 nmol), and 0.81 μg (1.75 nmol) for [^{11}C](±)-**12a**, [^{11}C](-)-**12a** and [^{11}C](+)-**12a**. In the displacement experiment, **6** (1 mg/kg, i.v.) was infused at 25 min after injection of [^{11}C](±)-**12a**. For this purpose, compound **6** was formulated in vehicle solution (8 mL) (saline/alcohol/cremophore EL, 9: 1: 0.1 by vol.). The solution was homogenized by vortexing and then passed through a sterile filter (0.2 μm pore size, Millex-GV, Millipore). The injected activity was 56 MBq with a specific radioactivity of 80.3 GBq/μmol. The mass of carrier associated with the injected radioactivity was 0.32 μg (0.70 nmol). The pre-block experiment was performed at 5 h after the baseline experiment. **6** was infused at 20 min before injection of radioligand. The injected activity was 57 MBq with specific radioactivities of 75.4 GBq/μmol. The mass of carrier associated with the injected radioactivity was 0.35 μg (0.76 nmol). In each PET experiment, scans were acquired in 3 frames over 93 min.

PET imaging

Radioactivity in brain was measured with the Siemens ECAT EXACT HR system. The three-ring detector block architecture gives a 15-cm wide field of view. All acquisitions were acquired in 3D-mode.44 The transversal resolution in the reconstructed image is about 3.8 mm full-width half-maximum (FWHM) and the axial resolution, 3.125 mm. The data were corrected for attenuation with three rotating ^{68}Ge rod sources. Raw PET data were then reconstructed using standard filtered back projection consisting of the following reconstruction parameters: 2-mm Hanning filter, scatter correction, a zoom factor of 2.17, and a 128 × 128 matrix size.44 Emission data were collected continuously for 93 min, according to a preprogrammed series of 20 frames starting immediately after i.v. injection of radioligand. The 3 initial frames were 1 min each, followed by 4 frames of 3 min each and 13 frames of 6 min each.

The mean image of the PET measurements (9-93 min) was transformed into a standard anatomical space using the monkey version of the Human Brain Atlas developed at the Karolinska Institutet.45 The transformation matrix generated on this image was applied to all frames of the corresponding baseline, displacement and pretreatment experiments. PET data were subsequently re-sliced to a resolution of 1.00, 1.00, 1.00 mm. Volumes of interest (VOIs) were manually defined on the coronal planes of an average monkey MRI. Similar VOIs were applied, as reported by Yasuno et al.,29 including cerebellum (1.9 cm^3), frontal cortex (7.4 cm^3), lateral temporal cortex (5.0 cm^3), medial temporal cortex (2.9 cm^3), striatum (2.1 cm^3), thalamus (0.9 cm^3) and pons (0.7 cm^3). Tissue radioactivity concentrations were expressed as % standardized uptake values (%SUV). Tissue radioactivity concentrations were decay-corrected and, in order to normalize for injected dose and body weight, expressed as % standardized uptake values (%SUV), where:

$$\%SUV=\left[\frac{\%\text{injected activity}}{\text{brain tissue}\,(g)}\times\text{body weight}\,(g)\right]$$

PET Plasma measurements

For radiometabolite measurements, venous blood (1 mL) was sampled from monkey at 5, 15, 30 and 45 min after injection of each radioligand. Plasma samples were measured as described previously.46 Briefly, the supernatant liquid (0.5 mL) obtained after centrifugation at 2000 × g for 1 min was mixed with MeCN (0.7 mL) containing standard (±)-**12a**. The supernatant liquid (1 mL) after another centrifugation at 2000 × g for 1 min was counted in a well counter and subsequently injected onto HPLC.

Supplementary Material

Refer to Web version on PubMed Central for supplementary material.

Acknowledgments

This work was supported by the Intramural Program of the National Institute of Mental Health (project # Z01-MH-002795). Mr. S.R. Donohue was also supported with a studentship under the NIH-Karolinska Institutet Graduate Training Partnership in Neuroscience. We thank other members of the PET group at the Karolinska Institutet for assistance. We are grateful to Eli Lilly and Co. for the provision of **6** under a CRADA (Cooperative Research and Development Agreement) with NIMH. We thank the NIMH Psychoactive Drug Screening Program (PDSP) and Marie Wennerberg at Astra Zeneca for performing binding assays. The PDSP is directed by Bryan L. Roth, Ph.D., with project officer Jamie Driscol (NIMH), at the University of North Carolina at Chapel Hill (contract NO1MH32004).

Abbreviations

ACS	American Chemical Society
AIDS	acquired immune deficiency syndrome
BSA	bovine serum albumin

CB_1	cannabinoid subtype-1
CB_2	cannabinoid subtype-2
CRADA	Cooperative Research and Development Agreement
DAT	dopamine transporter
DMSO	dimethyl sulfoxide
DOR	δ opioid receptor
DTT	dithiothreitol
ee	enantiomeric excess
EDTA	ethylene diamine tetraacetic acid
FWHM	full-width half-maximum
GTPγS	guanosine-5′-(γ-thio)-triphosphate
H	histamine receptor
HEPES	4-(2-hydroxyethyl)-1-piperazineethanesulfonic acid
HPLC	high-performance liquid chromatography
HRMS	high-resolution mass spectrometry
5-HT	5-hydroxytryptamine
K 2.2.2	4,7,13,16,21,24-hexaoxa-1,10-diazabicyclo[8.8.8]hexacosane
KI	Karolinska Institutet
KOR	κ opioid receptor
LC-MS	liquid chromatography-mass spectrometry
MeCN	acetonitrile
MOR	μ opioid receptor
MRI	magnetic resonance imaging
mp	melting point
MTBE	*tert*-butyl methyl ether
NET	norepinephrine transporter
NIH	National Institutes of Health
NIMH	National Institute of Mental Health
NMR	nuclear magnetic resonance
PDSP	Psychoactive Drug Screening Program
PET	positron emission tomography
PipISB	*N*-(4-fluoro-benzyl)-4-(3-(piperidin-1-yl)-indole-1-sulfonyl)benzamide

P-gp	permeability-glycoprotein
ppm	parts per million
SERT	serotonin transporter
SPECT	single-photon emission computed tomography
SUV	standardized uptake value
TEA	triethylamine
Δ^9-THC	Δ^9-tetrahydrocannabinol
VOI	volume of interest

References

(1). Vincent BJ, McQuiston DJ, Einhorn LH, Nagy CM, Brames MJ. Review of cannabinoids and their anti-emetic effectiveness. Drugs. 1983; 25:52–62. [PubMed: 6301800]

(2). Mackie K. Cannabinoid receptors as therapeutic targets. Annu. Rev. Pharmacol. Toxicol. 2005; 46:101–122. [PubMed: 16402900]

(3). Lambert DM, Fowler CJ. The endocannabinoid system: drug targets, lead compounds, and potential therapeutic applications. J. Med. Chem. 2005; 48:5059–5087. [PubMed: 16078824]

(4). Izzo AA, Coutts AA. Cannabinoids and the digestive tract. Handb. Exp. Pharmacol. 2005; 168:573–598. [PubMed: 16596788]

(5). Darmani NA, Crim JL. Δ^9-Tetrahydrocannabinol differentially suppresses emesis versus enhanced locomotor activity produced by chemically diverse dopamine D_2/D_3 receptor agonists in the least shrew (*Cryptotis parva*). Pharmacol. Biochem. Behav. 2005; 80:35–44. [PubMed: 15652378]

(6). Beal JE, Olson R, Laubenstein L, Morales JO, Bellman P, Yangco B, Lefkowitz L, Plasse TF, Shepard KV. Dronabinol as a treatment for anorexia associated with weight loss in patients with AIDS. J. Pain Symptom Manage. 1995; 10:89–97. [PubMed: 7730690]

(7). Beal JE, Olson R, Lefkowitz L, Laubenstein L, Bellman P, Yangco B, Morales JO, Murphy R, Powderly W, Plasse TF, Mosdell KW, Shepard KV. Long-term efficacy and safety of dronabinol for acquired immunodeficiency syndrome-associated anorexia. J. Pain Symptom Manage. 1997; 14:7–14. [PubMed: 9223837]

(8). Grundy RI. The therapeutic potential of the cannabinoids in neuroprotection. Expert Opin. Investig. Drugs. 2002; 11:1365–1374.

(9). Pryce G, Ahmed Z, Hankey DJ, Jackson SJ, Croxford JL, Pocock JM, Ledent C, Petzold A, Thompson AJ, Giovannoni G, Cuzner ML, Baker D. Cannabinoids inhibit neurodegeneration in models of multiple sclerosis. Brain. 2003; 126:2191–2202. [PubMed: 12876144]

(10). Gaoni Y, Mechoulam R. Isolation structure and partial synthesis of active constituent of hashish. J. Am. Chem. Soc. 1964; 86:1646–1647.

(11). Mechoulam R, Gaoni Y. The absolute configuration of Δ^1-tetrahydrocannabinol, the major active constituent of hashish. Tetrahedron. Lett. 1967; 12:1109–1111. [PubMed: 6039537]

(12). Devane WA, Dysarz FA, Johnson MR, Melvin LS, Howlett AC. Determination and characterization of a cannabinoid receptor in rat-brain. Molecular Pharmacology. 1988; 34:605–613. [PubMed: 2848184]

(13). Munro S, Thomas KL, Abushaar M. Molecular characterization of a peripheral receptor for cannabinoids. Nature. 1993; 365:61–65. [PubMed: 7689702]

(14). Shire D, Carillon C, Kaghad M, Calandra B, Rinaldicarmona M, Lefur G, Caput D, Ferrara P. An amino-terminal variant of the central cannabinoid receptor resulting from alternative splicing. J. Biol. Chem. 1995; 270:3726–3731. [PubMed: 7876112]

(15). Ryberg E, Vu HK, Larsson N, Groblewski T, Hjorth S, Elebring T, Sjorgren S, Greasley PJ. Identification and characterisation of a novel splice variant of the human CB_1 receptor. FEBS Lett. 2005; 579:259–264. [PubMed: 15620723]

(16). Herkenham M, Lynn AB, Little MD, Johnson MR, Melvin LS, Decosta BR, Rice KC. Cannabinoid receptor localization in brain. Proc. Natl. Acad. Sci. U.S.A. 1990; 87:1932–1936. [PubMed: 2308954]

(17). Herkenham M, Lynn AB, Johnson MR, Melvin LS, Decosta BR, Rice KC. Characterization and localization of cannabinoid receptors in rat brain: a quantitative in vitro autoradiographic study. J. Neurosci. 1991; 11:563–583. [PubMed: 1992016]

(18). Lynn AB, Herkenham M. Localization of cannabinoid receptors and nonsaturable high-density cannabinoid binding-sites in peripheral-tissues of the rat: implications for receptor-mediated immune modulation by cannabinoids. J. Pharmacol. Exp. Ther. 1994; 268:1612–1623. [PubMed: 8138973]

(19). Griffin G, Fernando SR, Ross RA, McKay NG, Ashford MLJ, Shire D, Huffman JW, Yu S, Lainton JAH, Pertwee RG. Evidence for the presence of CB_2-like cannabinoid receptors on peripheral nerve terminals. Eur. J. Pharmacol. 1997; 339:53–61. [PubMed: 9450616]

(20). Rinaldi-Carmona M, Barth F, Heaulme M, Shire D, Calandra B, Congy C, Martinez S, Maruani J, Neliat G, Caput D, Ferrara P, Soubrié P, Brelière J-C, Le Fur G. SR141716A, a potent and selective antagonist of the brain cannabinoid receptor. FEBS Lett. 1994; 350:240–244. [PubMed: 8070571]

(21). Lange JHM, Kruse CG, Tipker J, Tulp MTM, Van Vliet BJ. 4,5-Dihydro-1H-pyrazole derivatives having CB_1-antagonist activity. PTC Int. Appl. WO 0170700. 2001

(22). Lange JHM, Coolen H, van Stuivenberg HH, Dijksman JAR, Herremans AHJ, Ronken E, Keizer HG, Tipker K, McCreary AC, Veerman W, Wals HC, Stork B, Verveer PC, den Hartog AP, de Jong NMJ, Adolfs TJP, Hoogendoorn J, Kruse CG. Synthesis, biological properties, and molecular modeling investigations of novel 3,4-diarylpyrazolines as potent and selective CB_1 cannabinoid receptor antagonists. J. Med. Chem. 2004; 47:627–643. [PubMed: 14736243]

(23). Lange JHM, Kruse CG, Tipker J, Hoogendoorn J. 4,5-Dihydro-1H-pyrazole derivatives having CB_1-antagonist activity. PTC Int. Appl. WO 02076949. 2002

(24). Horti AG, Fan H, Kuwabara H, Hilton J, Ravert HT, Holt DP, Alexander M, Kumar A, Rahmim A, Scheffel U, Wong DF, Dannals RF. ^{11}C-JHU75528: A radiotracer for PET imaging of CB_1 cannabinoid receptors. J. Nucl. Med. 2006; 47:1689–1696. [PubMed: 17015906]

(25). Fan H, Ravert HT, Holt DP, Dannals RF, Horti AG. Synthesis of 1-(2,4-dichlorophenyl)-4-cyano-5-(4-[^{11}C]methoxyphenyl)-*N*-(piperidin-1-yl)-1*H*-pyrazole-3-carboxamide ([^{11}C]JHU75528) and 1-(2-bromophenyl)-4-cyano-5-(4-[^{11}C]methoxyphenyl)-*N*-(piperidin-1-yl)-1*H*-pyrazole-3-carboxamide ([^{11}C]JHU75575) as potential radioligands for PET imaging of cerebral cannabinoid receptor. J. Label. Compd. Radiopharm. 2006; 49:1021–1036.

(26). Donohue SR, Halldin C, Schou M, Hong J, Phebus LA, Chernet E, Hitchcock SA, Gardinier KM, Ruley KM, Krushinski JH, Schaus JM, Pike VW. Radiolabeling of a high potency cannabinoid subtype-1 receptor ligand, *N*-(4-fluoro-benzyl)-4-(3-(piperidin-1-yl)-indole-1-sulfonyl)benzamide (PipISB), with carbon-11 or fluorine-18. J. Label. Compd. Radiopharm. 2008; 51:146–152.

(27). Burns HD, Van Laere K, Sanabria-Bohorquez S, Hamill TG, Bormans G, Eng WS, Gibson R, Ryan C, Connolly B, Patel S, Krause S, Vanko A, Van Hecken A, Dupont P, De Lepeleire I, Rothenberg P, Stoch SA, Cote J, Hagmann WK, Jewell JP, Lin LS, Liu P, Goulet MT, Gottesdiener K, Wagner JA, de Hoon J, Mortelmans L, Fong TM, Hargreaves RJ. [^{18}F]MK-9470, a positron emission tomography (PET) tracer for i*n vivo* human PET brain imaging of the cannabinoid-1 receptor. Proc. Natl. Acad. Sci. U.S.A. 2007; 104:9800–9805. [PubMed: 17535893]

(28). Liu P, Lin LS, Hamill TG, Jewell JP, Lanza TJ, Gibson RE, Krause SM, Ryan C, Eng WS, Sanabria S, Tong XC, Wang JY, Levorse DA, Owens KA, Fong TM, Shen CP, Lao JL, Kumar S, Yin WJ, Payack JF, Springfield SA, Hargreaves R, Burns HD, Goulet MT, Hagmann WK. Discovery of *N*-{(1*S*,2*S*)-2-(3-Cyanophenyl)-3-[4-(2-[^{18}F]fluoroethoxy)phenyl]-1-methylpropyl}-2-methyl-2-[(5-methylpyridin-2-yl)oxy]propanamide, a cannabinoid-1 receptor positron emission tomography tracer suitable for clinical use. J. Med. Chem. 2007; 50:3427–3430. [PubMed: 17608398]

(29). Yasuno F, Brown AK, Zoghbi SS, Krushinski JH, Chernet E, Tauscher J, Schaus JM, Phebus LA, Chesterfield AK, Felder CC, Gladding RL, Hong J, Halldin C, Pike VW, Innis RB. The PET radioligand [^{11}C]MePPEP binds reversibly and with high specific signal to cannabinoid CB_1 receptors in nonhuman primate brain. Neuropsychopharmacology. 2008; 33:259–269. [PubMed: 17392732]

(30). Laruelle M, Slifstein M, Huang Y. Relationships between radiotracer properties and image quality in molecular imaging of the brain with positron emission tomography. Mol. Imaging Biol. 2003; 5:363–375. [PubMed: 14667491]

(31). Waterhouse RN. Determination of lipophilicity and its use as a predictor of blood-brain barrier penetration of molecular imaging agents. Mol. Imaging Biol. 2003; 5:376–389. [PubMed: 14667492]

(32). Andersson Y, Långström B. Transition metal-mediated reactions using [^{11}C]cyanide in synthesis of ^{11}C-labeled aromatic-compounds. J. Chem. Soc., Perkin Trans. 1. 1994; 11:1395–1400.

(33). Ponchant M, Hinnen F, Demphel S, Crouzel C. [^{11}C]Copper(I) cyanide: a new radioactive precursor for ^{11}C-cyanation and functionalization of haloarenes. Appl. Radiat. Isot. 1997; 48:755–762.

(34). Mathews WB, Monn JA, Ravert HT, Holt DP, Schoepp DD, Dannals RF. Synthesis of a $mGluR_5$ antagonist using [^{11}C]copper(I) cyanide. J. Label. Compd. Radiopharm. 2006; 49:829–834.

(35). Carson RE. PET physiological measurements using constant infusion. Nucl. Med. Biol. 2000; 27:657–660. [PubMed: 11091108]

(36). Jaffe H, Leffler JE. Synthesis of benziodathiazoles. J. Org. Chem. 1975; 40:797–799.

(37). Grosscurt AC, Vanhes R, Wellinga K. 1-Phenylcarbamoyl-2-pyrazolines, a New Class of insecticides. 3. Synthesis and insecticidal properties of 3,4-diphenyl-1-phenylcarbamoyl-2-pyrazolines. J. Agric. Food Chem. 1979; 27:406–409.

(38). Airaksinen AJ, Andersson J, Troung P, Karlsson O, Halldin C. Radiosynthesis of [^{11}C]ximelagatran via palladium catalyzed [^{11}C]cyanation. J. Label. Compd. Radioparm. 2008; 51:1–5.

(39). Cheng Y, Prusoff WH. Relationship between the inhibition constant (K_i) and the concentration of inhibitor which causes 50 per cent inhibition (IC_{50}) of an enzymatic reaction. Biochem. Pharmacol. 1973; 22:3099–108. [PubMed: 4202581]

(40). Christman DR, Finn RD, Karlstrom KI, Wolf AP. Production of ultra high activity ^{11}C-labeled hydrogen-cyanide, carbon-dioxide, carbon-monoxide and methane via ^{14}N(p,α)^{11}C reaction. Intl. J. Appl. Radiat. Isot. 1975; 26:435–442.

(41). Foged C, Halldin C, Hiltunen J, Braestrup C, Thomsen C, Hansen HC, Suhara T, Pauli S, Swahn CG, Karlsson P, Larsson S, Farde L. Development of ^{123}I-labelled NNC 13-8241 as a radioligand for SPECT visualization of benzodiazepine receptor binding. Nucl. Med. Biol. 1996; 23:201–209. [PubMed: 8782227]

(42). Clark, JD.; Baldwin, RL.; Bayne, KA.; Brown, MJ.; Gebhart, GF.; Gonder, JC.; Gwathmey, JK.; Keeling, ME.; Kohn, DF.; Robb, JW.; Smith, OA.; Steggerda, J-AD.; VandeBer, JL. Guide for Care and Use of Laboratory Animals. National Academies Press; Washington, DC: 1996.

(43). Karlsson P, Farde L, Halldin C, Swahn CG, Sedvall G, Foged C, Hansen KT, Skrumsager B. PET examination of [^{11}C]NNC-687 and [^{11}C]NNC-756 as new radioligands for the D_1-dopamine receptor. Psychopharmacology. 1993; 113:149–156. [PubMed: 7855175]

(44). Wienhard K, Dahlbom M, Eriksson L, Michel C, Bruckbauer T, Pietrzyk U, Heiss WD. The ECAT Exact HR: Performance of a new high-resolution positron scanner. J. Comp. Assist. Tomogr. 1994; 18:110–118.

(45). Roland PE, Graufelds CJ, Wåhlin J, Ingelman L, Andersson M, Ledberg A, Pedersen J, Åkerman S, Dabringhaus A, Zilles K. Human brain atlas: for high-resolution functional and anatomical mapping. Human Brain Mapping. 1994; 1:173–184. [PubMed: 24578038]

(46). Halldin, C.; Swahn, CG.; Farde, L.; Sedvall, G. Radioligand disposition and metabolism. In: Comar, D., editor. PET for Drug Development and Evaluation. Kluwer Academic Publishers; Dordrecht, Netherlands: 1995. p. 55-65.

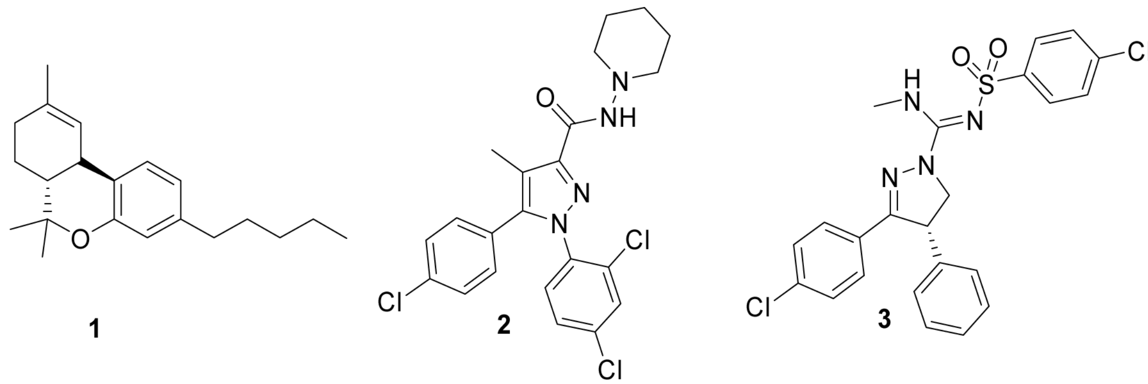

Figure 1.
Structures of CB_1 receptor ligands (**1-3**).

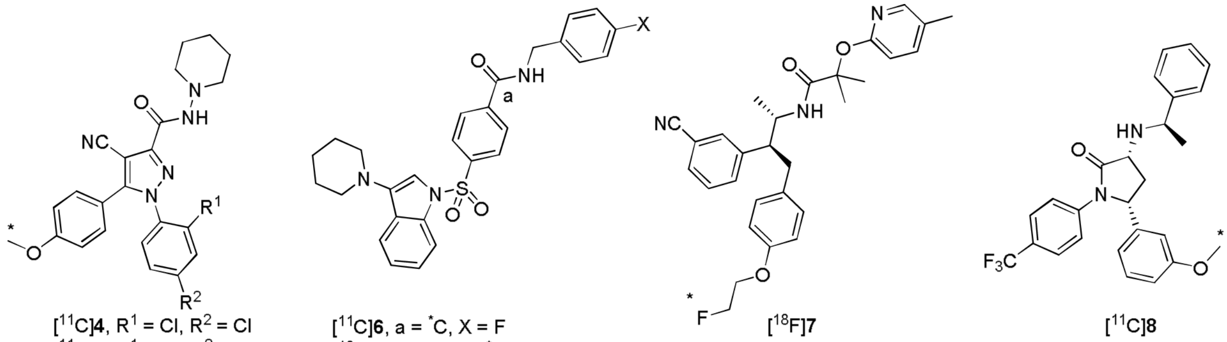

[^{11}C]**4**, R^1 = Cl, R^2 = Cl
[^{11}C]**5**, R^1 = Br, R^2 = H

[^{11}C]**6**, a = *C, X = F
[^{18}F]**6**, a = C, X = *F

[^{18}F]**7**

[^{11}C]**8**

Figure 2.
Structures of [^{11}C]**4-6**, [^{18}F]**6**, [^{18}F]**7** and [^{11}C]**8**.

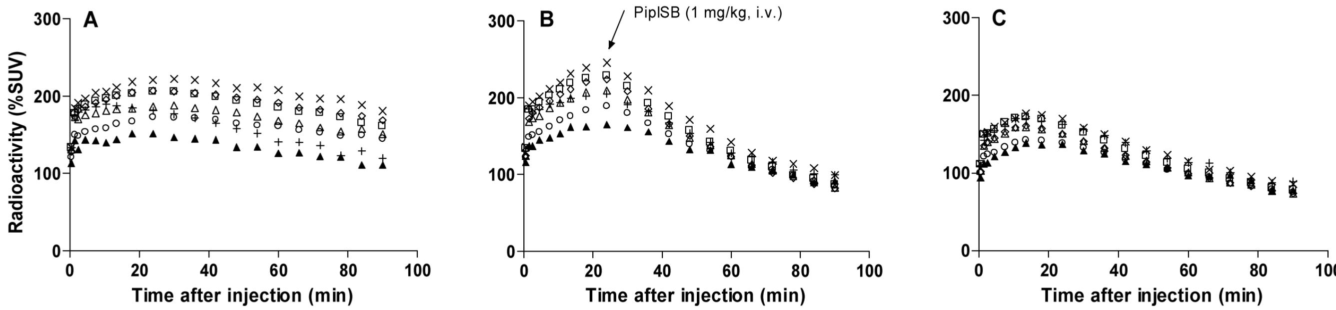

Figure 3.

Regional time-radioactivity curves after i.v. injection of [^{11}C](±)-**12a** in cynomolgus monkey under baseline condition (Panel A), with **6** (1 mg/kg, i.v.) administered as a displacing agent at 25 min (Panel B), or pretreatment condition with **6** (1 mg/kg, i.v.) (Panel C). Key: ×, striatum; △, cerebellum; ◇, frontal cortex; □, lateral temporal cortex; +, thalamus; ○, medial temporal cortex; ▲, pons.

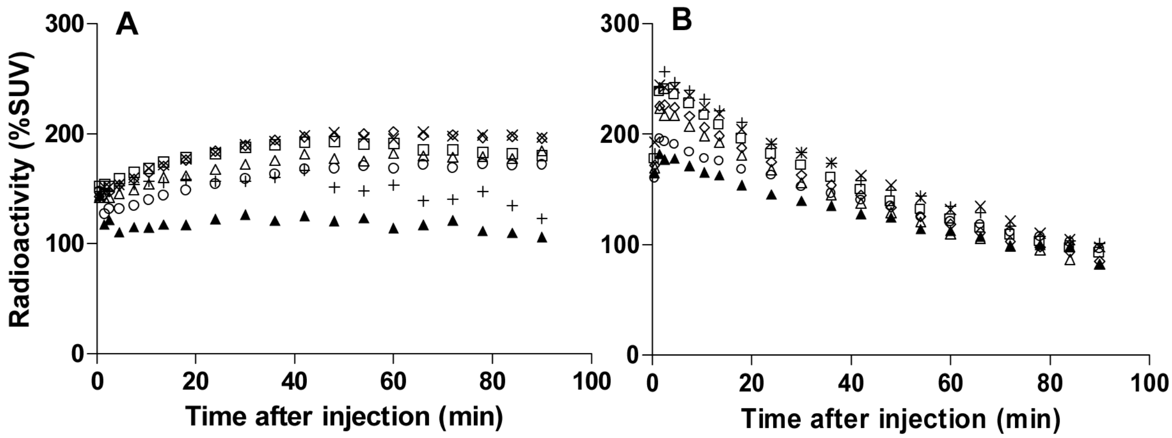

Figure 4.

Regional time-radioactivity curves after i.v. injection of [[11]C](-)-**12a** (100 MBq) (Panel A) or [[11]C](+)-**12a** (98 MBq) (Panel B) in cynomolgus monkey. Key: ×, striatum; △, cerebellum; ◇, frontal cortex; □, lateral temporal cortex; +, thalamus; ○, medial temporal cortex; ▲, pons.

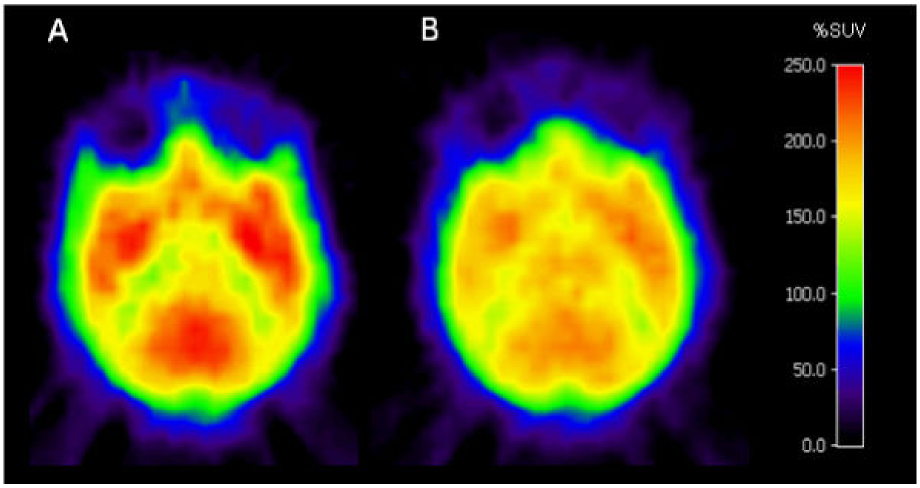

Figure 5.

Horizontal PET images, obtained at the level of the striatum from data acquired between 9 and 93 min after injection of [^{11}C](-)-**12a** (100 MBq, Panel A) or [^{11}C](+)-**12a** (98 MBq, Panel B).

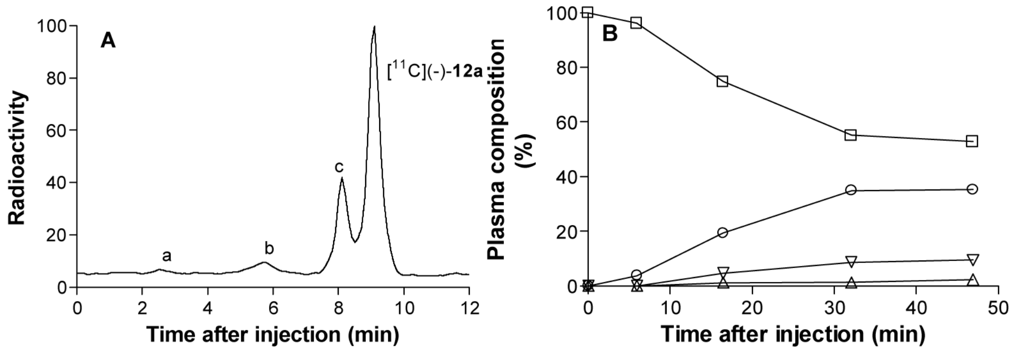

Figure 6.

Radio-HPLC of plasma of [^{11}C](-)-**12a** in cynomolgus monkey (15 min after injection, Panel A), and time course of radioactivity in plasma represented by parent radioligand and radiometabolite fractions (Panel B). Key: □, [^{11}C](-)-**12a**; △, metabolite a; ▽, metabolite b; ○, metabolite c.

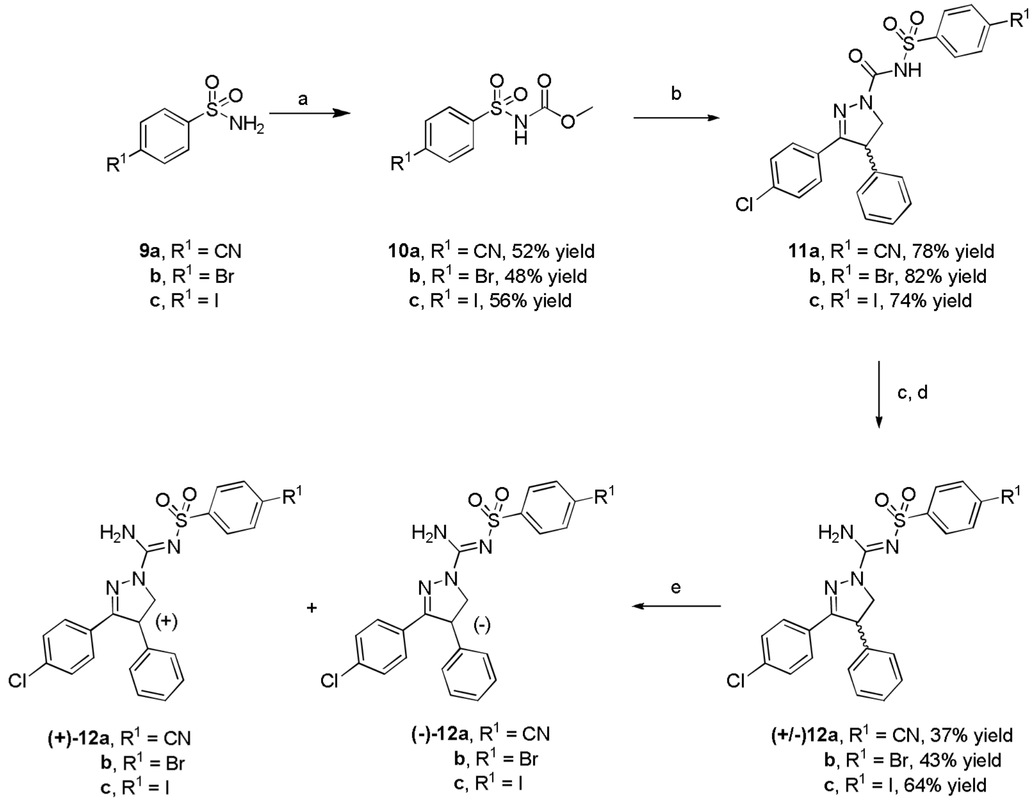

Scheme 1.

Synthesis of 3,4-diarylpyrazoline derivatives. Conditions: a) methyl chloroformate, TEA, MeCN; b) 3-(4-chlorophenyl)-4,5-dihydro-4-phenyl-1*H*-pyrazole, toluene, reflux; c) chlorobenzene, PCl_5; d) methanolic NH_3; e) ChiralPak AD, MeCN, 8 mL/min for **12a** and **12b** and 6 mL/min for **12c**.

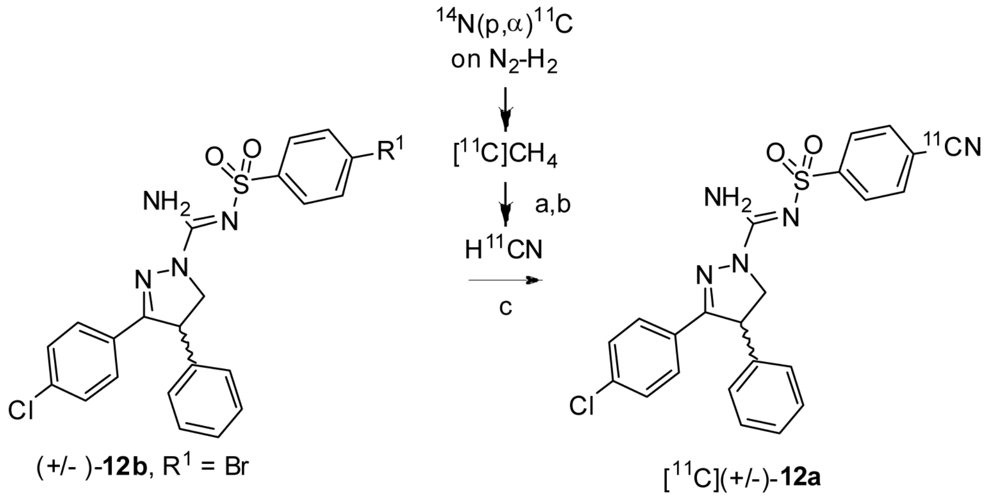

Scheme 2.

Radiosynthesis of $[^{11}C]$(±)-**12a**. Conditions, reagents and decay-corrected yield: a) Pt, NH_3 (20-30 mL/min), 990 °C. b) 50% H_2SO_4, 90 °C; c) $Pd(PPh_3)_4$, KOH, K2.2.2, DMSO, 110 °C, 36% (n = 2).

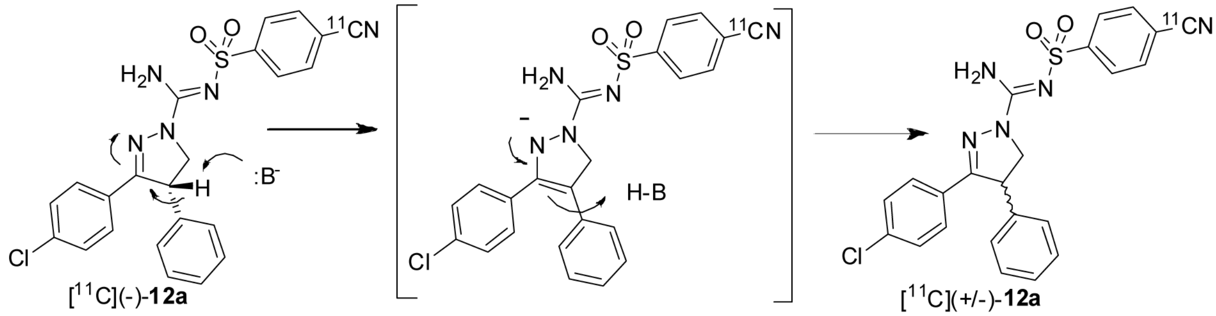

Scheme 3.

Proposed mechanism for the epimerization of [^{11}C](-)-**12a** under labeling conditions.

NIH-PA Author Manuscript
NIH-PA Author Manuscript

Table 1

IC_{50} and K_i values for the CBL_1 and CB_2 receptors and cLog*P* data for ligands **2**, (-)-**12a**, (+)-**12a**, (-)-**12c** and (+)-**12c**.

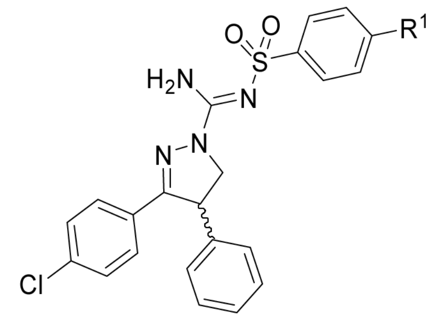

Ligand	R^1	CB_1 IC_{50} (nM)[a]	CB_2 IC_{50} (nM)[a]	CB_1 K_i (nM)[a]	CB_2 K_i (nM)[a]	cLog*P*[b]
2		2.2 ± 0.5	4,570 ± 410	0.4 ± 0.1	697 ± 63	6.95
(-)-**12a**	CN	2.8 ± 0.3	> 33,000	0.5 ± 0.1	> 5,000	3.85
(+)-**12a**	CN	100 ± 10	> 33,000	16.9 ± 2.0	> 5,000	3.85
(-)-**12c**	I	1.9 ± 0.7	> 33,000	0.3 ± 0.1	> 5,000	5.07
(+)-**12c**	I	103.5 ± 9.0	> 33,000	17.4 ± 2.0	> 5000	5.07

[a] Values are represent the mean ± SD of three determinations.

[b] cLog*P* values were calculated by using the Pallas 3.0 software (Compudrug, USA).

Table 2

Enantiomer composition (%) of [^{11}C]**12a** after treating (-)-**12b**, (-)-**12c** or (+)-**12c** with [^{11}C]cyanide ion in DMSO the presence of various bases

Precursor	Base (a)	[^{11}C](-)-12a (%)	[^{11}C](+)-12a (%)
(-)-**12b**	KOH, K2.2.2	50	50
	$NaHCO_3$	90	10
(-)-**12c**	NaOAc	50	50
	$NaHCO_3$	90	10
	KH_2PO_4	> 97 (*n* = 4)	< 3 (*n* = 4)
(+)-**12c**	KH_2PO_4	< 3 (*n* = 1)	> 97 (*n* = 1)